



Cite this: *RSC Adv.*, 2021, **11**, 32454

Received 13th July 2021  
 Accepted 14th September 2021  
 DOI: 10.1039/d1ra05376k  
[rsc.li/rsc-advances](http://rsc.li/rsc-advances)

## 1. Introduction

Radioactive waste is in general a burden to the public. Currently, the storage and/or disposal of large volumes of low- and intermediate-level radioactive liquid waste represents an issue of high concern.<sup>1–3</sup> The compaction of these large volumes, that comprise thousands of cubic meters, is highly desirable from both an environmental and an economical point of view. Among the different fission products in nuclear power reactors, cesium-137 (<sup>137</sup>Cs) is of particular importance. In fact, this radioactive isotope has a half-life of roughly 30 years, and it is both a beta- and a gamma-emitter.<sup>4</sup> As a result of its nuclear properties, <sup>137</sup>Cs is the primary source of penetrating gamma radiation for decades after discharge of, *e.g.*, spent nuclear fuel.<sup>5,6</sup> Similar to the other alkali metals, cesium is water-soluble and prone to bioaccumulation in marine and freshwater ecosystems due to its capability of substituting sodium and potassium in living organisms<sup>7–10</sup>. Ingestion of <sup>137</sup>Cs leads to the accumulation of this radioactive isotope in soft tissues from the thyroid, lungs, breast, and bone marrow,<sup>11–14</sup> resulting in a biological action similar to a continuous exposure to radiation from external sources. The ultimate effect of bioaccumulation of <sup>137</sup>Cs in humans, in dependency to the amount ingested, is

the development of radiation-induced malignancies,<sup>15–17</sup> as well as mutagenesis in germinal cells.<sup>18,19</sup> Many methods are currently available for decontamination of radioactive wastewater from nuclear fission products.<sup>20–27</sup> However, most of the existing technologies, like co-precipitation, evaporation, reverse osmosis, and ion exchange, show strong disadvantages, with the main ones being low efficiencies, high production and operational costs, or limited reusability. Clay minerals (*e.g.*, zeolite, bentonite, vermiculite, and montmorillonite) suffer from the competitive interactions of sodium and potassium with the available adsorption sites. The consequences are slow kinetics and/or poor selectivity.<sup>28,29</sup> Furthermore, avoiding the production of toxic derivatives and residues from the decontamination process is of utmost importance.

In this work, we exhibit the potential of a new filter material, based on a blend of whey-protein fibrils and active charcoal,<sup>30</sup> for the treatment of radioactive aqueous waste deriving from nuclear industry and other radiochemical activities. Previously, this filter membrane demonstrated to remove a wide variety of contaminants from wastewaters, under diverse chemical conditions.<sup>30–34</sup> The surprisingly broad retention capacity of this material offers thus excellent prospects for the decontamination of radioactive aqueous waste deriving from nuclear power industry, radionuclide production, as well from nuclear medicine. In this study, we focused our attention in the treatment of wastewater containing <sup>137</sup>Cs, since an effective removal of this problematic fission product can be considered as a benchmark for the successful application of the above-mentioned filtering material in the cleaning of low-to medium-level radioactive aqueous waste containing other fission products (*e.g.*, <sup>90</sup>Sr).

First, we synthesized the amyloids–carbon hybrid membranes as indicated in ref. 30. Then, preliminary tests on the performance of the filter material regarding the removal of

<sup>a</sup>Laboratory of Radiochemistry, Paul Scherrer Institute, Villigen PSI 5232, Switzerland.  
 E-mail: nadine-mariel.chiera@psi.ch

<sup>b</sup>BluAct Technologies GmbH, Glattpark 8152, Switzerland

<sup>c</sup>Department of Health Sciences and Technology, ETH Zürich, Zürich 8092, Switzerland. E-mail: raffaele.mezzenga@hest.ethz.ch

<sup>d</sup>Department of Chemistry and Applied Biosciences, ETH Zürich, Zürich 8092, Switzerland

<sup>e</sup>Department of Materials, ETH Zürich, Zürich 8092, Switzerland

† These authors contributed equally to this work.



$^{137}\text{Cs}$  from radioactive samples in aqueous phase were conducted. The average  $^{137}\text{Cs}$  activity per unit volume of each test sample amounted to  $2.5 \cdot 10^5 \text{ Bq L}^{-1}$ . This is comparable to the maximum concentration of  $^{137}\text{Cs}$  in the seawater just off the accident site of the Fukushima Daichii Nuclear Power Plant one month after the accident, *i.e.*,  $10^5 \text{ Bq L}^{-1}$ .<sup>35</sup> In an initial set of adsorption experiments, we investigated the interaction of trace amounts (*i.e.*, carrier free) of ionic  $^{137}\text{Cs}$  with the protein-bearing filter membrane at zero surface coverage. A successive set of experiments included the addition of weighable amounts of  $^{nat}\text{CsCl}$  with admixtures of the radioactive tracer  $^{137}\text{Cs}$ , enabling us to explore the sorption capacity of this amyloid–carbon hybrid filtering material. The latter is a decisive parameter for a potential industrial application. Gamma-ray spectrometry was applied for measuring the activity of  $^{137}\text{Cs}$  before and after filtration of the contaminated water samples. Finally, the homogeneity of the distribution of the retained  $^{137}\text{Cs}$  in the filter material was investigated by autoradiography.

## 2. Experimental

### 2.1. Preparation of the hybrid membrane

Whey protein isolate ( $\beta$ -lactoglobulin) was purchased from Bipro @Agropure. The preparation of the amyloid fibrils was carried out without any further purification by heat denaturation of the 2 wt% monomer solution at pH 2 for 5 hours. Activated carbon (Norit carbon, particle diameter less than 60 mesh) was utilized. Hybrid composite membranes having 10 wt% amyloid fibrils were prepared by initial mixing of  $\beta$ -lactoglobulin solution, activated carbon and paper pulp in the ratio of 10 : 40 : 50 wt% respectively, as well as cellulose as supporting material. Water was removed from this mixture by vacuum filtration followed by a pressing and drying process similar to paper manufacturing. The obtained membranes (3 mm in thickness) were cropped to disks with a diameter of 50 mm and finally used to filter the radioactive water samples containing  $^{137}\text{Cs}$ . The characteristics of the membrane are found in Table 1.

### 2.2. Preparation of the aqueous carrier-free and carrier-added $^{137}\text{Cs}$ -solutions

Aqueous samples containing tracer amounts of  $^{137}\text{Cs}$  were prepared by diluting an aliquote (100  $\mu\text{L}$ ) of a stock solution of  $^{137}\text{CsCl}$  to 50 mL with MilliQ-2 water. Each test solution was then acidified to a pH = 4 using 1 M HCl in order to mimic a corrosive environment. Aqueous samples containing macroscopic amounts of CsCl were obtained by preparation of a 10 ppm  $^{nat}\text{CsCl}$  (analytical grade EMSURE®, Merck KGaA) aqueous solution (50 mL in volume), to which 100  $\mu\text{L}$  of the above-mentioned  $^{137}\text{CsCl}$  stock solution were added. It should

be noted here that the addition of the  $^{137}\text{Cs}$  tracer does not change the overall concentration of the carrier-added cesium solution with a concentration of 10 ppm. The  $^{137}\text{CsCl}$  stock solution was obtained from the large-scale research facility Hotlab at Paul Scherrer Institute, Switzerland. All solutions were prepared using ultrapure water, obtained from the MilliQ-2 system water purifier (Millipore Corp., Bedford, USA). The mineral acid was of ACS grade, and procured from Sigma-Aldrich (HCl, 37%). Each test solution showed an average activity in the range of 10–12 kBq, *i.e.*, an activity concentration of approx.  $2.5 \cdot 10^5 \text{ Bq L}^{-1}$ . The pH of each test solution was determined using pH indicator strips MColorpHast™ (pH 0–14). Aliquots of various volumes of the test solutions were used for filtration.

### 2.3. Filtration procedure

Experiments were conducted with the syringe-aided setup shown in Fig. 1a. The synthesized hybrid membrane filter was placed inside the filter holder (Fig. 1b and c). The edges of the screwcap of the adaptor were greased with silicone lubricant to ensure a leak-proof and tight fit. Before filtration of the radioactive samples, the membranes were conditioned with MilliQ-2 water (5 mL) acidified with HCl to a pH  $\approx$  4. After the pre-treatment of the filter, the radioactive test solutions were passed through the filtration cell by applying gentle pressure with the syringe at a flux of approx.  $1 \text{ mL min}^{-1}$ .

### 2.4. Gamma-ray spectroscopy

The monitoring and quantification of the amount of  $^{137}\text{Cs}$  in each sample was done by integrating the total number of counts in the main gamma-line of  $^{137}\text{Cs}$  at 662 keV. Gamma-spectroscopy measurements were performed with a Broad Energy Germanium (BEGe) detector (Canberra, Mirion Technologies, Inc.). All the solutions were measured in a defined geometry using HDPE scintillation vials. The energy calibration

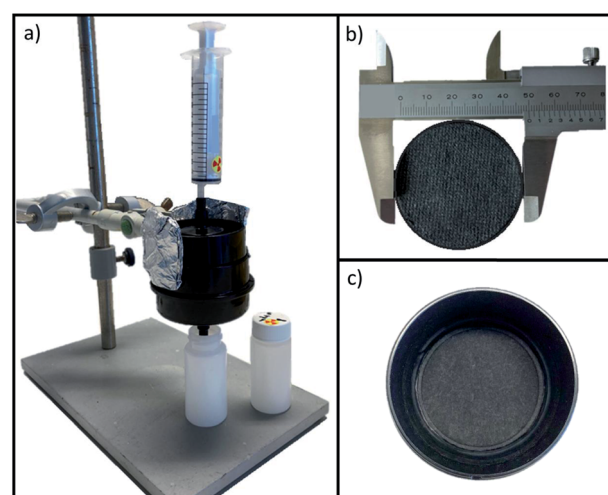


Fig. 1 (a) Syringe-aided filtration setup for the removal of  $^{137}\text{Cs}$  from aqueous samples; (b) top view of filter disk (50 mm diameter); (c) top-down view of the filter holder containing the amyloid–carbon hybrid filter.

Table 1 Characteristics of the membrane

Protein content	10 wt%
Activated carbon total surface area (BET)	$1150 \text{ m}^2 \text{ g}^{-1}$
Thickness of membrane	3 mm
Membrane pore size	0.7 $\mu\text{m}$



of the spectrometer was done with a certified  $^{152}\text{Eu}$  standard reference gamma-source from PTB (Physikalisch-Technische Bundesanstalt), Braunschweig, Germany. The efficiency calibration of the spectrometer was performed with a  $^{133}\text{Ba}$  liquid calibration source with a specific activity of  $2 \text{ Bq } \mu\text{L}^{-1}$ . The determination of this specific activity itself was determined by using a certified source of  $^{133}\text{Ba}$  (PTB). All gamma-spectra were recorded and analyzed with the Genie 2000 Gamma Analysis software (Canberra, Mirion Technologies, Inc.).

## 2.5. Radiographic imaging

The homogeneity of the distribution of the retained  $^{137}\text{Cs}$  was investigated by autoradiography. A GE Typhoon FLA 7000 IP imaging plate scanner, equipped with a BAS-IP MS 2040 E super resolution film was used to obtain the autoradiographic images. The filters were placed over the film for 72 hours, and the data were analyzed with the ImageJ software (U. S. National Institutes of Health, Maryland, USA, <https://imagej.nih.gov/ij>).

## 2.6. Safety and protection measures

The assessment of the adverse effects upon exposure (by ingestion or inhalation) to materials containing pathological amyloid fibrils is still under study.<sup>36-38</sup> At present, global safety guidelines and/or protocols for handling this type of material are not yet fully defined. However, there start to be converging opinions that the use of food-based amyloids, as in the present case, is safe for human consumption.<sup>39</sup> Therefore, in our studies, we applied the same ALARA (As Low As Reasonably Achievable) safety concept that is applied when handling radioactive material. Synthesis, characterization, and experiments with the filters containing the amyloid fibrils and the radioactive material were conducted in a variable air volume fume hood, wearing protective nitrile gloves (EN ISO 374-1 and EN ISO 374-5 type), laboratory face masks (KN95 lab grade), and safety eyewear (EN 166, EN 169, and EN 170 standards). For further radiochemical safety, the dose rate (below the  $\mu\text{Sv h}^{-1}$  level) was measured at the working distance using dose rate meters 6150AD® Automation und Messtechnik GmbH. The personnel was equipped with personal dosimeters for the detection of gamma, beta, and neutron radiation.

## 3. Results and discussion

The gamma-spectrometric measurements demonstrated that after a single filtration cycle the  $^{137}\text{Cs}$  content in 20 mL of radioactive water is reduced by a factor of approx. 340 to about  $700 \text{ Bq L}^{-1}$ , with a decontamination efficiency of 99.7% (see Fig. 2a). According to the International Commission on Radiological Protection,<sup>40</sup> the guidance level value of  $^{137}\text{Cs}$  in drinking water is  $10 \text{ Bq L}^{-1}$ . Hence, two consecutive filtering cycles are sufficient to render an initial sample of radioactively contaminated water suitable for human consumption. To clarify the role played by the amyloid fibrils in the adsorption process, retention experiments were performed with the same typology and mesh-size of filter support deprived of the amyloid–carbon hybrid admixture. As shown in Fig. 2b, the retention of  $^{137}\text{Cs}$

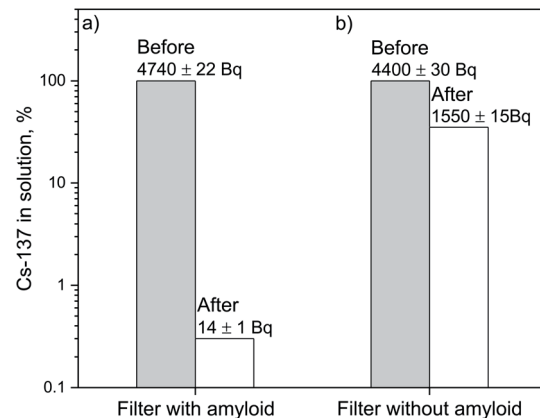


Fig. 2 Activity of  $^{137}\text{Cs}$  in [Bq] before and after the filtration of a radioactive aqueous sample (volume = 20 mL) through (a) an amyloid–carbon hybrid membrane, (b) a quartz fibre membrane.

without the amyloid–carbon hybrid filter is about 100 times less efficient, clearly indicating that the protein aggregates are the main contributors to the chemical binding and retention of Cs.

The uptake of cations by the filter material originates from a supramolecular interaction between the cation and the  $\beta$ -sheets of the  $\beta$ -lactoglobulin amyloid fibrils, stabilized by the presence of multiple amino-acid residues.<sup>32,41</sup> As shown in previous studies, the strongest binding motif of the  $\beta$ -lactoglobulin protein sequence is the 121-cys residue containing the amyloidogenic fragment LACQCL.<sup>30,42,43</sup>

Radiographic imaging of the amyloid–carbon hybrid filter (Fig. 3) shows the spatial distribution of  $^{137}\text{Cs}$  as captured in the membrane. The homogenous distribution indicates no preferential flow paths of the liquid through the filtration unit. The observed darker spots in Fig. 3 are due to accumulation of activity caused by

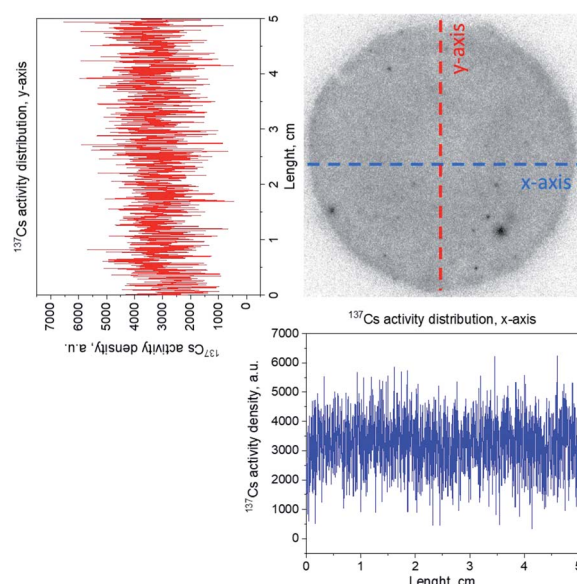


Fig. 3 Radiographic image of the amyloid–carbon hybrid filter after uptake of  $^{137}\text{Cs}$ . The distribution of  $^{137}\text{Cs}$  along the x- and the y-axis is shown.



the rough nature of the filtering material itself. The retention capacity of the membrane was investigated by performing consecutive filtrations of carrier-added CsCl solutions (10 ppm) spiked with  $^{137}\text{Cs}$  for monitoring purposes, at a flux of approx.  $1 \text{ mL min}^{-1}$ . Six consecutive filtration cycles of a total volume of 30 mL led to a total uptake of 102  $\mu\text{g}$  of Cs, without reaching saturation (see Fig. 4). This indicates a specific sorption capacity of at least 36  $\mu\text{g}$  of Cs per gram of filter material, at the applied conditions.

The fitting of the data points in Fig. 4 was performed by applying an asymptotic regression model, as described in ref. 44:

$$y = a - bc^x \quad (1)$$

The method defines a limited growth, where  $y$  represents the cumulative retention of Cs by the filter, and  $x$  equals to the cumulative addition of Cs in the filter itself. The parameter  $a$  represents the asymptotic value with respect to  $y$ ;  $b$  is the change in  $y$  when  $x$  passes from 0 to infinity; and  $c$  is the factor by which the difference ( $y-a$ ) is reduced by increasing  $x$ . For the value of  $c$  the constrain  $0 < c < 1$  holds. In our experiments, for  $x = 0$  (*i.e.*, no Cs added to the filter), then it is obtained  $y = 0$  (*i.e.*, no Cs retained in the filter). This condition is true only if  $a = b$ . Hence, eqn (1) can be re-written as follows:

$$y = a(1 - c^x) \quad (2)$$

The fitting of the data with the Origin® 2018 software package, yields:

$$a = 142.4(36) \mu\text{g}$$

$$c = 0.9925(3)$$

The curve asymptote  $a$  (*i.e.*, the value at which the quantity of Cs retained by the filter reaches a plateau), represents the

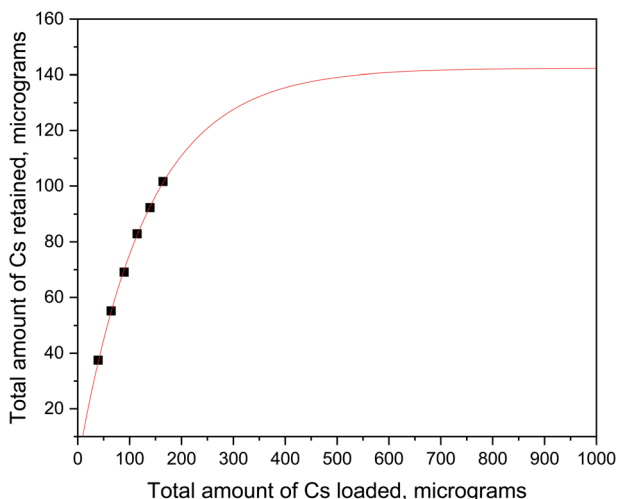


Fig. 4 Cumulative retention of macroscopic amounts of CsCl solution (10 ppm) spiked with  $^{137}\text{Cs}$ , during a consecutive series of filtrations (squares) using 2.8 g of filter material (10 wt% protein fibrils). Data fitting of the saturation-type plot is indicated (solid line); errors of data points are too small to be shown.

Table 2 Cesium sorption capacities of diverse filter materials at pH = 4 and  $T = 25^\circ\text{C}$ . Abbreviations: c.t. (contact time), a.c. (adsorption strongly affected by competing ions)

Adsorbent	Adsorption capacity ( $\text{mg g}^{-1}$ )	Notes	Ref.
KNiFC <sup>a</sup>	0.123	7 days c.t.	45
Clinoptilolites	1.31	48 h c.t.	46
$\text{MnO}_2\text{-PAN}^b$	0.942	35 min c.t.; a.c.	47
Cellulose + gypsum	0.5	10 days c.t.	48
Bentonite	0.54	7 h c.t.; a.c.	49
HMO <sup>c</sup>	0.11	25 min c.t.	50
HSO <sup>d</sup>	0.12	20 min c.t.	50
Amyloid fibrils	0.62	~6 min c.t.	This work

<sup>a</sup> Potassium nickel hexacyanoferrate loaded-silica gels and chabazite.

<sup>b</sup> PAN = polyacrylonitrile. <sup>c</sup> Hydrous manganese oxide. <sup>d</sup> Hydrous stannic oxide.

saturation limit of Cs for a 2.28 g filter containing 10 wt% of  $\beta$ -lactoglobulin fibrils. This gives an estimated maximum sorption capacity of 0.62 mg of Cs per gram of amyloid fibrils. For comparison, the Cs adsorption capacities of various materials at pH = 4 and at room temperature are listed in Table 2.

Based on these results, it is expected that radioactivity levels up to 0.2 TBq (*i.e.*, in the order of  $10^{11}$  decays per second) per kg of filter material can be extracted from radioactively contaminated water in a single filtration step. Different experimental settings of, *e.g.*, contact time and pH of the filtered water may further influence the observed sorption capacity. Investigations on the reversibility of the retention process may define the maximum volume of liquid allowed per filter mass – a parameter that will greatly depend as well on the geometry of the filter arrangements optimized for industrial processing.

## 4. Conclusions

The studied hybrid membrane is an efficient filtration material for the decontamination of low-to medium-level radioactive wastewater from  $^{137}\text{Cs}$ . The application of this filter material for the removal of other fission products from radioactive aqueous waste is envisaged. Further investigations on the stability of the amyloid fibrils against radiation damage (*i.e.*, degeneration of the protein-based binding sites) will help to understand whether this filter material can be efficiently applied in the treatment of high-level radioactive liquid wastes as well. Since the membranes are made completely from natural components, its controlled combustion to ashes further minimizes the final radioactive waste volume. These results may lead to an inexpensive and environmentally sustainable technology for the treatment of radioactive waste from various sources, including nuclear power plants.

## Conflicts of interest

R. M. and S. B. are the inventors of a filed patent application related to the work presented here. All the other authors declare no competing interests.



## Notes and references

1 M. I. Ojovan, R. A. Robbins and M. Garamszeghy, *MRS Adv.*, 2018, **3**, 983–990.

2 R. Pusch, J. Kasbohm, S. Knutsson, T. Hoang-Minh and L. Nguyen-Thanh, *J. Earth Sci. Geotech. Eng.*, 2019, **9**, 237–272.

3 L. Abrahamsen-Mills and J. S. Small. Organic-containing nuclear wastes and national inventories across Europe, in *The Microbiology of Nuclear Waste Disposal*, Elsevier, 2021, pp. 1–20.

4 J. Magill and R. Dreher, *AIP Conf. Proc.*, 2009, **1164**, 100–106, <http://www.nucleonica.net>.

5 S. Vaccaro, S. Tobin, A. Favalli, B. Grogan, P. Jansson, H. Liljenfeldt, V. Mozin, J. Hu, P. Schwalbach, A. Sjöland and H. Trellue, *Nucl. Instrum. Methods Phys. Res., Sect. A*, 2016, **833**, 208–225.

6 J. Bruno and R. Ewing, *Elements*, 2006, **2**, 343–349.

7 C. R. Bader and D. Bertrand, *J. Physiol.*, 1984, **347**, 611–631.

8 P. M. Hughes and A. D. Macknight, *J. Physiol.*, 1977, **267**, 113–136.

9 A. J. Levi, J. S. Mitcheson and J. C. Hancox, *J. Physiol.*, 1996, **492**, 1–9.

10 T. A. Baramanda, R. Bakri and H. Suseno, *IOP Conf. Ser.: Mater. Sci. Eng.*, 2020, **902**, 012056.

11 Y. I. Bandazhevsky, *Swiss Med. Wkly.*, 2003, **133**, 35–36.

12 A. V. Nesterenko, V. B. Nesterenko and A. V. Yablokov, in *Chernobyl: Consequences of the Catastrophe for People and the Environment*, ed. A. V. Yablokov, V. B. Nesterenko, A. V. Nesterenko and J. D. Sherman-Nevinger, Annals of the New York Academy of Sciences, Boston, 2010, **26**, p. 289.

13 E. R. Svendsen, I. E. Kolpakov, Y. I. Stepanova, V. Y. Vdovenko, M. V. Naboka, T. A. Mousseau, L. C. Mohr, D. G. Hoel and W. J. Karmaus, *Environ. Health Perspect.*, 2010, **118**, 720–725.

14 M. Izawa and H. Tsubota, *J. Radiat. Res.*, 1962, **3**, 120–129.

15 R. M. Rahal, M. E. Rocha, R. Freitas-Junior, R. da Silveira Corrêa, D. Rodrigues, E. Martins, L. R. Soares and J. C. Oliveira, *Asian Pac. J. Cancer Prev.*, 2019, **20**, 3811.

16 Y. Shimizu, H. Kato, W. J. Schull and D. G. Hoel, *Radiat. Res.*, 1992, **130**, 249–266.

17 D. A. Pierce and D. L. Preston, *Radiat. Res.*, 2000, **154**, 178–186.

18 E. O. Alves Costa, D. de Melo e Silva, A. V. de Melo, F. Ribeiro Godoy and H. F. Nunes, *Mutagenesis*, 2011, **26**, 651–655.

19 A. D. a Cruz, D. D. a Silva, C. C. da Silva, R. J. Nelson, L. M. Ribeiro, E. R. Pedrosa, J. C. Jayme and M. P. Curado, *Mutat. Res., Genet. Toxicol. Environ. Mutagen.*, 2008, **652**, 175–179.

20 X. Zhang, P. Gu and Y. Liu, *Chemosphere*, 2019, **215**, 543–553.

21 M. Lin, I. Kajan, D. Schumann and A. Türler, *J. Radioanal. Nucl. Chem.*, 2019, **322**, 1857–1862.

22 D. Rana, T. Matsuura, M. Kassim and A. Ismail, *Desalination*, 2013, **321**, 77–92.

23 M. Jiménez-Reyes, P. Almazán-Sánchez and M. Solache-Ríos, *J. Environ. Radioact.*, 2021, **233**, 106610–106622.

24 X. Zhang and Y. Liu, *Environ. Sci.: Nano*, 2020, **7**, 1008–1040.

25 Z. X. Wu Y, W. YZ and M. H, *Sep. Purif. Technol.*, 2017, **181**, 76–84.

26 O. Halevi, T. Chen, P. Lee, S. Magdassi and J. Hriljac, *RSC Adv.*, 2020, **10**, 5766–5776.

27 H. Faghihian, M. Iravani, M. Moayed and M. G. Maragheh, *Chem. Eng. J.*, 2013, **222**, 41–48.

28 O. Ararema, F. Bouras and F. Arbaoui, *Chem. Eng. J.*, 2011, **172**, 230–236.

29 E. H. Borai, R. Harjula and A. Paajanen, *J. Hazard. Mater.*, 2009, **172**, 416–422.

30 S. Bolisetty and R. Mezzenga, *Nat. Nanotechnol.*, 2016, **11**, 365–371.

31 S. Bolisetty, N. Reinhold, C. Zeder, M. Orozco and R. Mezzenga, *Chem. Commun.*, 2017, **53**, 5714–5717.

32 M. Peydayesh, S. Bolisetty, T. Mohammadi and R. Mezzenga, *Langmuir*, 2019, **35**, 4161–4170.

33 S. Bolisetty, N. Coray, A. Palika, G. Prenosil and R. Mezzenga, *Environ. Sci.: Water Res. Technol.*, 2020, **6**, 3249–3254.

34 A. Palika, A. Armanious, A. Rahimi, C. Medaglia, M. Gasbarri, S. Handschin, A. Rossi, M. Pohl, I. Busnadiego, C. Gübeli and R. Anjanappa, *Nat. Nanotechnol.*, 2021, **16**, 918–925.

35 H. Kaeriyama, *Fish. Oceanogr.*, 2017, **26**, 99–103.

36 V. Bellotti, M. Nuvolone, S. Giorgetti, L. Obici, G. Palladini, P. Russo, F. Lavatelli, V. Perfetti and G. Merlini, *Ann. Med.*, 2007, **39**, 200–207.

37 S. Tsukawaki, T. Murakami, K. Suzuki and Y. Nakazawa, *Biomed. Mater.*, 2016, **11**, 065010–065018.

38 V. Bellotti and F. Chiti, *Curr. Opin. Struct. Biol.*, 2008, **18**, 771–779.

39 Y. Cao and R. Mezzenga, *Adv. Colloid Interface Sci.*, 2019, **269**, 334–356.

40 A. Wrixon, *J. Radiol. Prot.*, 2008, **28**, 161–168.

41 I. Javed, Y. Sun, J. Adamcik, B. Wang, A. Kakinen, E. H. Pilkington, F. Ding, R. Mezzenga, T. P. Davis and P. C. Ke, *Biomacromolecules*, 2017, **18**, 4316–4322.

42 J. H. Viles, *Coord. Chem. Rev.*, 2012, **256**, 2271–2284.

43 J. Park, W. Lee, G. Lee, H. Choi, M. Kim, W. Kim, S. Na and J. Park, *J. Electrochem. Soc.*, 2019, **166**, B1497.

44 W. L. Stevens, *Biometrics*, 1951, **7**, 247.

45 H. Mimura, M. Kimura, K. Akiba and Y. Onodera, *Solvent Extr. Ion Exch.*, 1999, **17**, 403–417.

46 A. Abusafa and H. Yücel, *Sep. Purif. Technol.*, 2002, **28**, 103–116.

47 A. Nilchi, R. Saberi, S. R. Garmarodi and A. Bagheri, *Appl. Radiat. Isot.*, 2012, **70**, 369–374.

48 M. Y. Miah, K. Volchek, W. Kuang and F. H. Tezel, *J. Hazard. Mater.*, 2010, **183**, 712–717.

49 A. F. Seliman, Y. F. Lasheen, M. A. E. Youssief, M. M. Abo-Aly and F. A. Shehata, *J. Radioanal. Nucl. Chem.*, 2014, **300**, 969–979.

50 S. P. Mishra, *Sep. Purif. Technol.*, 2007, **54**, 10–17.

